Molecular Biology of the Cell
Vol. 19, 3203–3211, August 2008

Elucidation of a TRPC6-TRPC5 Channel Cascade That Restricts Endothelial Cell Movement

Pinaki Chaudhuri,* Scott M. Colles,* Manjunatha Bhat,† David R. Van Wagoner,‡ Lutz Birnbaumer,§ and Linda M. Graham*‖

*Department of Biomedical Engineering, †Center for Anesthesiology Research, ‡Department of Molecular Cardiology, and ‖Department of Vascular Surgery, Cleveland Clinic, Cleveland, OH 44195; and §National Institute of Environmental Health Sciences, Research Triangle Park, NC 27709

Submitted August 8, 2007; Revised April 23, 2008; Accepted May 8, 2008
Monitoring Editor: John York

Canonical transient receptor potential (TRPC) channels are opened by classical signal transduction events initiated by receptor activation or depletion of intracellular calcium stores. Here, we report a novel mechanism for opening TRPC channels in which TRPC6 activation initiates a cascade resulting in TRPC5 translocation. When endothelial cells (ECs) are incubated in lysophosphatidylcholine (lysoPC), rapid translocation of TRPC6 initiates calcium influx that results in externalization of TRPC5. Activation of this TRPC6–5 cascade causes a prolonged increase in intracellular calcium concentration ($[Ca^{2+}]_i$) that inhibits EC movement. When TRPC5 is down-regulated with siRNA, the lysoPC-induced rise in $[Ca^{2+}]_i$ is shortened and the inhibition of EC migration is lessened. When TRPC6 is down-regulated or EC from *TRPC6*$^{-/-}$ mice are studied, lysoPC has minimal effect on $[Ca^{2+}]_i$ and EC migration. In addition, TRPC5 is not externalized in response to lysoPC, supporting the dependence of TRPC5 translocation on the opening of TRPC6 channels. Activation of this novel TRPC channel cascade by lysoPC, resulting in the inhibition of EC migration, could adversely impact on EC healing in atherosclerotic arteries where lysoPC is abundant.

INTRODUCTION

Many endothelial cell (EC) functions, including EC migration, are regulated by the influx of calcium ion (Ca^{2+}) through calcium channels (Tran *et al.*, 1999; Isshiki *et al.*, 2002; Chaudhuri *et al.*, 2003). EC monolayer disruption causes influx of Ca^{2+} from the extracellular milieu and a rise in intracellular Ca^{2+} concentration ($[Ca^{2+}]_i$) that is required for initiation of movement (Tran *et al.*, 1999). Elevated $[Ca^{2+}]_i$ causes detachment of focal adhesions and cytoskeletal changes. After the initial rise in $[Ca^{2+}]_i$, caveolae and the machinery for calcium wave initiation relocate to the trailing edge of the cell (Isshiki *et al.*, 2002). This may allow new focal adhesions to assemble in the leading portion of the cell. Sustained increase in $[Ca^{2+}]_i$, such as that induced by lysophosphatidylcholine (lysoPC), a phospholipid abundant in the plasma and atherosclerotic lesions (Portman and Alexander, 1969; Subbaiah *et al.*, 1985), disrupts time- and site-specific changes in focal adhesions and cytoskeleton that are required for cell movement and thus inhibits EC migration to repair monolayer disruption (Chaudhuri *et al.*, 2003).

This article was published online ahead of print in *MBC in Press* (http://www.molbiolcell.org/cgi/doi/10.1091/mbc.E07–08–0765) on May 21, 2008.

Address correspondence to: Linda M. Graham (grahamL@ccf.org).

Abbreviations used: AS, antisense oligonucleotide; $[Ca^{2+}]_i$, intracellular calcium concentration; ECs, endothelial cells; lysoPC, lysophosphatidylcholine; MAECs, mouse aortic ECs; Scr, scrambled oligonucleotide; TRP, transient receptor potential (protein); TRPC, canonical transient receptor potential (protein); *TRPC6*$^{-/-}$, TRPC6 deficient.

Multiple distinct calcium entry pathways are present in ECs, including receptor-operated channels and store-operated Ca^{2+} channels. A major class of cation channels are homologues of the transient receptor potential (TRP) channels in *Drosophila*. These can be receptor-operated channels, store-operated channels, or both. The TRP family has at least 21 members, and all TRP subfamilies, including canonical (TRPC), vanilloid, and melastatin, are represented in ECs (Nilius and Droogmans, 2003). The seven TRPC channels are divided into two groups based on their homology and mechanism of activation. TRPC1, TRPC4, and TRPC5 have been characterized as store-dependent channels and TRPC3, TRPC6, and TRPC7 as store-independent channels, but at least TRPC3, TRPC5, and TRPC7 are recognized to function as both receptor- and store-operated channels (Nilius and Droogmans, 2003; Lièvremont *et al.*, 2004; Zeng *et al.*, 2004). Although all TRPC channels are expressed in EC (Yip *et al.*, 2004), expression varies in different vascular beds (Yao and Garland, 2005), and this may influence EC function.

Previous studies in our laboratory showed that lysoPC's inhibitory effect on EC migration was due in part to increased calcium entry through store-independent, non-voltage-gated calcium channels (Chaudhuri *et al.*, 2003), but the channels involved were not identified. LysoPC activated TRPC5 channels in HEK cells overexpressing TRPC5 (Flemming *et al.*, 2006) and increased $[Ca^{2+}]_i$ in smooth muscle cells that have endogenous TRPC6 channels (So *et al.*, 2005). Because TRPC5 and TRPC6 are expressed in bovine ECs (Yip *et al.*, 2004) and can be store-independent (Nilius and Droogmans, 2003; Zeng *et al.*, 2004) and because TRPC6 plays a role in vascular endothelial growth factor–mediated microvessel permeability and thrombin-induced EC shape change (Pocock *et al.*, 2004; Singh *et al.*, 2007), we explored

the role of TRPC5 and TRPC6 in lysoPC-induced calcium influx and subsequent inhibition of EC migration.

Here, we provide evidence that activation of TRPC5 and TRPC6 plays a critical role in lysoPC-induced calcium entry and inhibition of migration. In ECs, lysoPC activation of TRPC5 is dependent on TRPC6. In genetically modified ECs that do not express TRPC6, lysoPC does not induce calcium influx and has limited effect on EC migration. Our results suggest that lysoPC induces a cascade of events, including the opening of TRPC6 channels and activation of TRPC5, which results in sustained calcium entry from the extracellular medium that is responsible for inhibition of EC migration.

MATERIALS AND METHODS

EC Culture and Cell Migration Study

Bovine aortic ECs were isolated from adult bovine aortas by scraping after collagenase treatment. ECs between passage 4 and 10 were grown in DME with Ham's F12 nutrient mixture (1:1 vol/vol) containing 10% fetal calf serum (Hyclone Laboratories, Logan, UT). ECs were made quiescent in serum-free DME with 0.1% gelatin for 24 h before migration assay. EC migration was studied using the razor-scrape method as previously described (Chaudhuri *et al.*, 2003). Migrating cells were quantitated by an observer blinded to the experimental condition using NIH Image software (http://rsb.info.nih.gov/ij/).

Mouse aortic endothelial cells (MAECs) were harvested from wild-type (WT) and TRPC6-deficient (*TRPC6*$^{-/-}$) mice (Dietrich *et al.*, 2005). The Institutional Animal Care and Use Committee approved the proposed study. Mice were anesthetized by intraperitoneal injection of ketamine (80 mg/kg) and xylazine (5 mg/kg). MAECs were isolated following the method of Shi *et al.* (2000) with modification of the culture medium. Briefly, the aorta was removed, cut into rings, and placed into Matrigel in tissue culture wells. After 2–3 d, ECs growing from aortic rings were plated into a six-well plate coated with 0.2% gelatin and cultured in M199 medium with Ham's F12 nutrient mixture (4:1) with 10% fetal bovine serum (FBS) and gentamicin (1 μg/ml medium). EC identity was confirmed by immunostaining with anti-human von Willebrand Factor polyclonal antibody (1:100, Dako, Carpinteria, CA). Passage 3 or 4 MAECs were used in the experiments.

Immunoprecipitation of Total Proteins

Confluent ECs were either washed in tissue culture medium or incubated overnight in serum-free DME containing 0.1% gelatin, before treatment. After treatment, cells were harvested by scraping in cold lysis buffer. Insoluble material was removed, and soluble protein was measured. Samples containing equal amount of protein were incubated with the antigen-specific antibody overnight at 4°C. Protein A-G plus agarose beads were added for 2 h. Beads were collected by pulse centrifugation, washed with cold lysis buffer, resuspended in 40 μl 2× Laemmli buffer, and boiled. Proteins were separated by 4–12% gradient SDS-PAGE.

Immunoblot Analysis of Total Proteins

Lysates were stored at −20°C until analyzed. Proteins (50 μg/lane) were resolved by 4–12% gradient SDS-PAGE, transferred to a polyvinylidene difluoride membrane, and detected by antibodies specific for TRPC6 (1:250, Sigma, St. Louis, MO), TRPC3 (1:250, Sigma), TRPC5 (1:250, Sigma), or phosphotyrosine (1:1000, Santa Cruz Biotechnology, Santa Cruz, CA). The signal was developed using a chemiluminescent reagent (Perkin Elmer-Cetus, Boston, MA), and band density was quantitated using NIH Image software. To confirm equal loading, membranes were reprobed for actin (Chemicon, Temecula, CA).

Biotinylation of Proteins on EC Cell Surface

EC surface proteins were biotinylated as described by Cayouette *et al.* (2004). Briefly, ECs were grown in 60-mm dishes, treated as appropriate, washed with cold PBS, and incubated with 2 mg/ml Sulfo-NHS-SS-Biotin (Calbiochem, La Jolla, CA) for 30 min at 4°C. Biotinylation was terminated by washing with cold buffer containing 10 mM glycine. Cells were lysed in buffer (50 mM HEPES, 150 mM NaCl, 1 mM EDTA, 200 μM Na_3VO_4, 100 mM NaF, 1% Triton X-100, pH 7.4) containing protease inhibitors (Complete, Roche, Indianapolis, IN) for 30 min at 4°C. Lysates were passed through 20- and 25-gauge needles, cleared by centrifugation, and incubated with streptavidin-agarose beads for 18 h at 4°C. Biotin-streptavidin complexes were collected, washed, resuspended in 2× Laemmli buffer, and incubated at 60°C for 30 min. Proteins were resolved by SDS-PAGE and immunoblotting.

TRPC6 and TRPC5 Externalization by Immunofluorescence Analysis

ECs were grown on 25-mm coverslips until ~60% confluence, either immediately washed or made quiescent for 24 h, and then incubated with lysoPC (12.5 μM) or PBS. Cells were fixed in 100% methanol for 10 min at 4°C, then washed, blocked in 3% BSA for 1 h, and then incubated with anti-TRPC6 antibody (1: 100) or anti-TRPC5 antibody (1:100) for 2 h, followed by Alexa 488–conjugated donkey anti-rabbit antibody (Invitrogen, Carlsbad, CA; 1:1000) for 2 h. The nuclei were stained with 2 μg/ml propidium iodide (Sigma) for 30 min. The coverslips were mounted using Vectashield reagent (Vector Laboratories, Burlingame, CA) and viewed using a Leica fluorescence microscope (Heidelberg, Germany).

Overexpression of TRPC6 in ECs

ECs at 60% confluence were transiently transfected with 2 μg plasmids of pcDNA3-human TRPC6-eYFP or pcDNA3-human TRPC6 using Effectene (Qiagen, Chatsworth, CA) according to the manufacturer's protocol. The effectiveness of transfection was verified after 48 h by fluorescence microscopy and immunoblot analysis of TRPC6.

Electrophysiology

Whole cell currents were recorded from control ECs and from ECs transiently transfected with pcDNA3-human TRPC6-eYFP or pcDNA3-human TRPC6, using an Axopatch 200A amplifier and pClamp 9 software (Molecular Devices, Sunnyvale, CA). Patch pipettes with resistance of 2.5–5 MΩ were made using Corning 8161-thin wall glass (Warner Instruments, Hamden, CT). After establishing the whole cell configuration, currents were recorded at room temperature before and after the application of lysoPC (10 μM). The holding potential was adjusted to −60 mV, and voltage ramps from +60 to −100 mV over 140 ms were applied to the cell. Data were filtered at 2 kHz and sampled at 10 kHz. The standard external buffer containing 140 mM NaCl, 5.4 mM KCl, 2 mM $CaCl_2$, 1 mM $MgCl_2$, and 10 mM glucose, and 10 mM HEPES at pH 7.3 was used as the bath solution. The buffer for pipette solution contained 150 mM CsAsp, 10 mM NaOH, 1 mM $MgCl_2$, 0.1 mM EGTA, 5 mM Mg-ATP, and 10 mM HEPES at pH 7.2.

$[Ca^{2+}]_i$ Measurement

Calcium-binding fluorophore fura 2-AM was used for estimation of $[Ca^{2+}]_i$ as previously described (Chaudhuri *et al.*, 2003). Briefly, ECs were cultured in 35-mm dishes designed for fluorescence microscopy (Bioptechs, Butler, PA), loaded with fura 2-AM (1 μM) for 30 min and then washed with Krebs-Ringer (KR) buffer (125 mM NaCl, 5 mM KCl, 1.2 mM $MgSO_4$, 11 mM glucose, 2.5 mM $CaCl_2$, and 25 mM HEPES, pH 7.4) to remove excess fura 2-AM. Fluorescence of a group of 10–12 cells located inside the light path was continuously monitored with an Olympus 1X-70 inverted fluorescence microscope (Melville, NY). The relative change of $[Ca^{2+}]_i$ was determined using the ratio of fura-2 fluorescence intensity at excitation wavelengths of 340 and 380 nm (340/380 ratio).

Down-regulation of TRPC mRNA

ECs were transiently transfected with small interfering RNA (siRNA) to decrease TRPC5 mRNA levels. The specific targeted sequence of TRPC5 was sense, 5′-GGAGGCUGAGAUCUACUAUtt-3′; and antisense, 5′-AUAGUAGAUCUCAGCCUCCtg-3′ (Liu *et al.*, 2006). ECs at 80% confluence were incubated with siRNA duplex of TRPC5 (20 nM final concentration) for 24 h using the transfection kit (RNAiFect, Qiagen) and following the manufacturer's protocol. An siRNA (Ambion , Austin, TX) that has no homology to any known gene sequence was used as negative control. The effectiveness of TRPC5 siRNA to knock down endogenous TRPC5 level was verified after 48 h by immunoblot analysis of TRPC5.

ECs were transiently transfected with phosphorothioate-modified oligonucleotides (Integrated DNA Technologies, Coralville, IA) to decrease TRPC6 mRNA levels. Oligonucleotides corresponded to antisense, 5′-GTGAAGGAGGCTGCGTGTGC-3′; sense, 5′-GCACACGCAGCCTCCTTCAC-3′; or scrambled, 5′-GGCGTTATCAGGTGGAGGGC-3′ sequences based on conserved regions in the mouse and human TRPC6 sequences (Welsh *et al.*, 2002). ECs at 80% confluence were transiently transfected with 2 μg of phosphorothioate-modified oligonucleotide using Effectene (Qiagen) according to the manufacturer's protocol. The effectiveness of antisense oligonucleotides was verified after 48 h by immunoblot analysis of TRPC6.

Statistical Analysis

Data are represented as the mean ± SD unless otherwise noted. Experiments were done in triplicate with ECs from at least three different animals, and all blots shown in figures are representative of at least three experiments. Student's *t* test or ANOVA was used for analysis of data, and differences were considered statistically significant at $p < 0.05$.

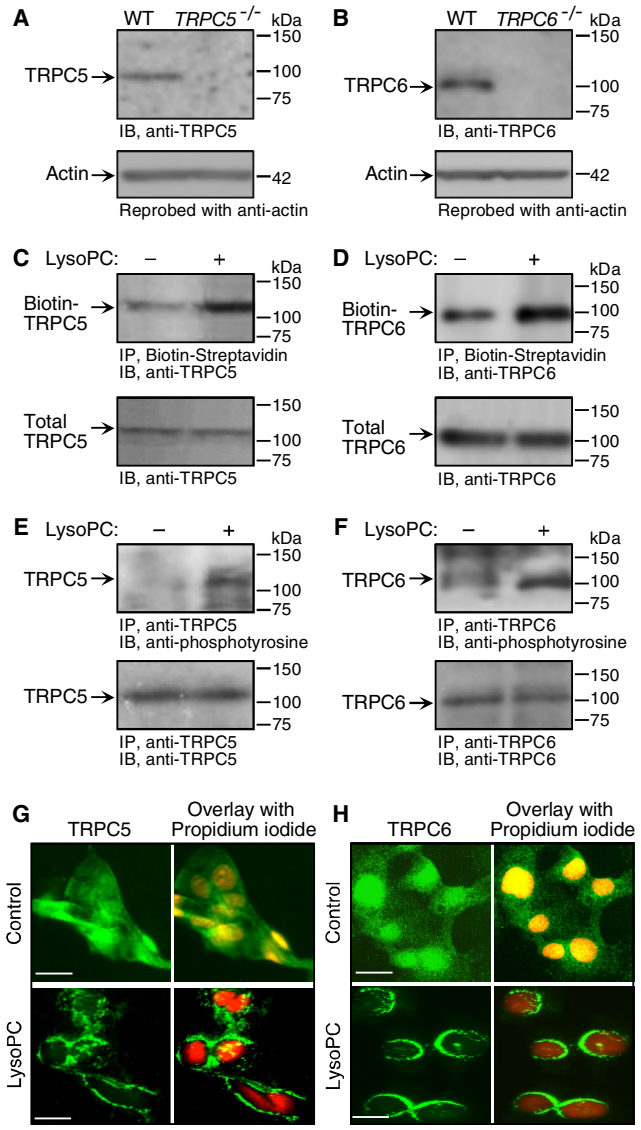

Figure 1. Translocation of TRPC5 and TRPC6 is induced by lysoPC. (A) Total protein was extracted from skeletal muscle tissues from wild-type (WT) and *TRPC5*$^{-/-}$ mice. Immunoblot analysis was performed to confirm the specificity of the anti-TRPC5 antibody. (B) Aortic ECs from wild-type and *TRPC6*$^{-/-}$ mice were lysed and immunoblot analysis was performed for total TRPC6 (n = 3) to confirm the specificity of the anti-TRPC6 antibody. (C) ECs were incubated with lysoPC for 1 h. Cell surface proteins were biotinylated, and immunoblot analysis performed for biotinylated TRPC5 (top panel). Before incubation with streptavidin-agarose beads, an aliquot of cell lysate was removed for immunoblot analysis to determine total TRPC5 (bottom panel). (D) Using similar methods, biotinylated TRPC6 (top panel) and total TRPC6 (bottom panel) were identified. (E) ECs were incubated with lysoPC for 1 h. TRPC5 was immunoprecipitated and immunoblot analysis was performed for phosphotyrosine (top panel) or total TRPC5 (bottom panel). (F) Using similar methods, tyrosine phosphorylated TRPC6 (top panel) and total TRPC6 (bottom panel) were identified. Representative blots of at least three separate experiments are shown in C–F. (G) At 60% confluence, ECs were made quiescent for 24 h, treated with or without lysoPC for 15 min, and then incubated with anti-TRPC5 antibody followed by Alexa 488–conjugated secondary antibody. TRPC5 location was assessed by fluorescence microscopy. Nuclei were detected by counterstaining with propidium iodide. (H) Using similar methods with anti-TRPC6 antibody, TRPC6 externalization was assessed by immunofluorescence microscopy. The images of TRPC5 (G) or TRPC6 (H) in ECs are the representative of four randomly chosen fields from each of three experiments. Original magnification, ×40. Bar, 40 μm.

RESULTS

LysoPC Activates TRPC5 and TRPC6

The effect of lysoPC (1-palmitol-2-hydroxy-*sn*-glycerol-3-phosphocholine; Avanti Polar Lipids, Alabaster, AL) on TRPC5 and TRPC6 channels was assessed in bovine aortic ECs. Initially, the specificity of anti-TRPC5 and anti-TRPC6 antibodies was validated using tissue from *TRPC5*$^{-/-}$ mice and *TRPC6*$^{-/-}$ mice (Figure 1, A and B). Then the ability of lysoPC to induce externalization of TRPC5 and TRPC6 in ECs was assessed using a biotinylation assay. LysoPC induced a 2.24 ± 0.4-fold increase in TRPC5 externalized to the EC plasma membrane (n = 3, $p < 0.01$, Figure 1C). Immunoblot analysis of EC lysates showed no change in total TRPC5, suggesting that the increase of TRPC5 at the plasma membrane surface was due to externalization of existing protein and not an increase in total TRPC5 (n = 3). TRPC6 on the plasma membrane surface increased 2.1 ± 0.5-fold after EC incubation with lysoPC for 1 h (n = 3, $p < 0.02$, Figure 1D). Surface TRPC6 returned to control levels by 24 h (data not shown). Western blot analysis of cell lysates showed no change in total TRPC6 (n = 3), suggesting that the increase in TRPC6 on the plasma membrane surface was due to externalization of existing protein and not an increase in total TRPC6. Tyrosine phosphorylation can modulate TRPC channel activity (Hisatsune *et al.*, 2004; Odell *et al.*, 2005). In ECs incubated with lysoPC (12.5 μM) for 1 h, a 3.4 ± 0.6-fold increase in tyrosine phosphorylation of TRPC5 was detected by immunoblot analysis (n = 3, $p < 0.01$, Figure 1E), and a 4.4 ± 1.3-fold (n = 3, $p < 0.01$) increase in tyrosine phosphorylation of TRPC6 was detected (Figure 1F). Because TRPC6 shares 75% amino acid identity to TRPC3 and TRPC7 (Boulay *et al.*, 1997; Okada *et al.*, 1999), lysoPC's effect on phosphorylation of TRPC3 channels was evaluated. TRPC3 tyrosine phosphorylation did not change (data not shown), suggesting that lysoPC did not have a generalized effect on all TRPC channels.

LysoPC-induced translocation of TRPC6 and TRPC5 to the EC plasma membrane was confirmed using fluorescence microscopy after immunostaining with anti-TRPC5 and anti-TRPC6 antibodies and fluorescent-labeled secondary antibody. Under control conditions, the pattern of TRPC5 (n = 3, Figure 1G, top panel) and TRPC6 (n = 3, Figure 1H, top panel) protein fluorescence was diffuse throughout the cytoplasm, although both appeared to be more concentrated in the nuclear region. After incubation with lysoPC, TRPC5 (n = 3, Figure 1G, bottom panel) and TRPC6 (n = 3, Figure 1H, bottom panel) fluorescence was associated with the plasma membrane, again suggesting that TRPC5 and TRPC6 translocated to the membrane. Immunostaining for TRPC6 was homogenous in the region of the plasma membrane, whereas that for TRPC5 appeared to be clustered.

The time course of channel externalization after addition of lysoPC was assessed (Figure 2, A and B). TRPC6 became externalized immediately after ECs were exposed to lysoPC (Figure 2B). On the other hand, TRPC5 externalization was delayed until ~3 min after addition of lysoPC (Figure 2A). These findings suggest that the time course of translocation, and thus the mechanism responsible, is different for TRPC5 and TRPC6. The same time course of TRPC5 and TRPC6 translocation was seen in ECs made quiescent in serum-free medium (data now shown).

LysoPC has been shown to activate TRPC5 channels in HEK-293 cells stably expressing tetracycline-regulated TRPC5 (Flemming *et al.*, 2006). To confirm that lysoPC also activates TRPC6 channels, changes in membrane current were assessed in normal ECs and ECs overexpressing

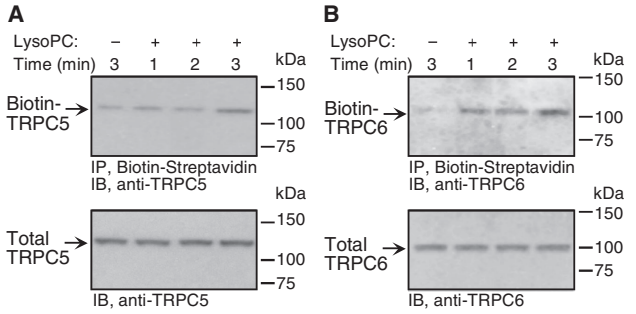

Figure 2. TRPC6 is externalized more rapidly than TRPC5 after incubation with lysoPC. (A) ECs were grown to confluence in 10% FBS, washed, incubated with or without lysoPC for 1, 2, or 3 min. Cell surface proteins were biotinylated and immunoblot analysis performed for biotinylated TRPC5. Before incubation with streptavidin-agarose beads, an aliquot of cell lysate was removed for immunoblot analysis to determine total TRPC5. (B) Again using a biotinylation assay, the time course of TRPC6 externalization after addition of lysoPC was determined. Total TRPC6 was determined by immunoblot analysis. Representative blots of at least three separate experiments are shown in A and B.

TRPC6 using whole cell patch-clamp technique. The effectiveness of transient transfection of TRPC6 was verified by immunoblot analysis (n = 4, Figure 3A). Current was measured before and immediately after addition of lysoPC when a rapid rise was seen in $[Ca^{2+}]_i$ (Chaudhuri *et al.*, 2003) and TRPC6 was externalized (Figure 2B). As shown in Figure 3, the electrophysiologic studies showed that lysoPC induced an increase in membrane current in control ECs and an even greater response in ECs overexpressing TRPC6. The peak current density (expressed as pico-amperes/pico-Faraday, pA/pF) rose significantly after addition of lysoPC to control ECs or ECs overexpressing TRPC6 (Figure 3D). Because TRPC6 level in the specific cell used in each electrophysiologic study could not be quantitated, lysoPC-induced membrane current could not be expressed as a function of TRPC6 channel number. In the current-voltage relationship (Figure 3B), the time plot (Figure 3C), and the peak current density (Figure 3D), a larger lysoPC-induced membrane current was noted in EC overexpressing TRPC6 than in control ECs. Taken together, the data suggested that lysoPC not only induced translocation of TRPC6 channels to the cell membrane, but induced functional current in EC overexpressing TRPC6.

LysoPC-induced $[Ca^{2+}]_i$ Rise and Inhibition of EC Migration Is Attenuated in TRPC6$^{-/-}$ MAECs

To further study the role of the TRPC6 channel in lysoPC-induced $[Ca^{2+}]_i$ rise and inhibition of migration, EC were harvested from aortas of *TRPC6*$^{-/-}$ mice. Immunoblot analysis showed no detectable TRPC6 in ECs from the *TRPC6*$^{-/-}$ mice (Figure 1B). Basal migration of wild-type and *TRPC6*$^{-/-}$ MAECs was similar (Figure 4A). After incubation in lysoPC (10 μM), wild-type MAEC migration was inhibited to 30% of baseline (n = 3, $p < 0.0001$ compared with untreated), but *TRPC6*$^{-/-}$ MAEC migration was 71% of baseline ($p < 0.0001$ compared with wild-type MAECs in lysoPC). Although lysoPC caused a prolonged rise in $[Ca^{2+}]_i$ in wild-type MAECs (n = 4), it had no effect on $[Ca^{2+}]_i$ in TRPC6-deficient ECs (n = 4, Figure 4B). This confirmed a role of TRPC6 channels in lysoPC-induced $[Ca^{2+}]_i$ rise and inhibition of EC migration.

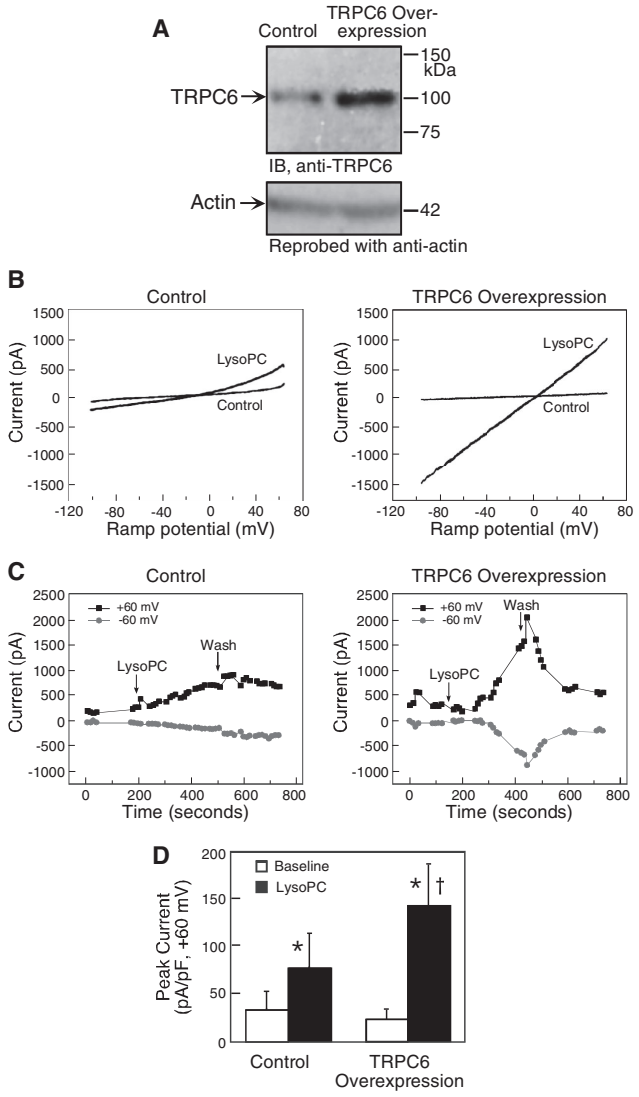

Figure 3. Overexpression of TRPC6 amplifies the response of bovine aortic ECs to lysoPC. (A) ECs were transiently transfected with pcDNA3-TRPC6 for 24 h, made quiescent for an additional 24 h, and then lysed. Immunoblot analysis was performed for TRPC6 (top panel) and the blot was reprobed for actin to confirm equal loading (bottom panel). (B) For study of current–voltage relationships, ECs were transiently transfected with pcDNA3-TRPC6-eYFP or pcDNA-TRPC6 for 24 h and then made quiescent for 24 h. Ramp current traces (+60 to −100 mV over 125 ms) were obtained in whole cell patch-clamp studies using control ECs with empty expression vector pcDNA3 (left panel) and ECs overexpressing TRPC6 (right panel). Control trace represents the last trace before application of lysoPC. The bath solution was changed to one containing lysoPC (10 μM), and data collection was continued. (C) The time plots of current traces from the ECs shown in B are depicted for control ECs (left panel) and ECs overexpressing TRPC6 (right panel). After obtaining a stable baseline, the bath solution was changed to one containing 10 μM lysoPC (arrow). After ~4 min, the bath solution was again changed to buffer without lysoPC (Wash), whereas data collection continued. (D) The peak current density (expressed as pico-amperes/pico-Faraday) was determined at baseline and after addition of lysoPC in five control ECs and seven ECs overexpressing TRPC6. The graph represents the mean ± SEM. $^*p < 0.05$ compared with baseline and $^{\dagger}p = 0.07$ compared with lysoPC-treated control ECs. (B and C) Representative of results obtained from five control ECs and seven ECs overexpressing TRPC6.

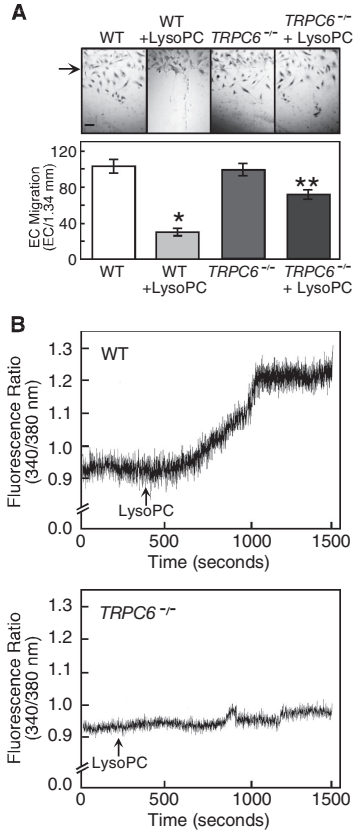

Figure 4. LysoPC has little effect on $[Ca^{2+}]_i$ or migration of *TRPC6*$^{-/-}$ MAECs. (A) ECs were grown to confluence and made quiescent for 12 h, and then the migration assay was initiated in the presence or absence of lysoPC (10 μM). The arrow indicates the starting line of migration. Original magnification, ×40. Bar, 100 μm. The bottom panel depicts migration results represented as mean ± SD (n = 3; * $p < 0.001$ compared with WT control and ** $p < 0.001$ compared with *TRPC6*$^{-/-}$ control). (B) MAECs were loaded with fura 2-AM. After adjusting the baseline, lysoPC (10 μM) was added to cells (arrow), and relative change of $[Ca^{2+}]_i$ was monitored in WT (top panel) and *TRPC6*$^{-/-}$ MAECs (bottom panel). Each trace is representative of four separate experiments.

TRPC5 or TRPC6 Down-Regulation Prevented Increased $[Ca^{2+}]_i$ and Preserved EC Migration during Incubation with LysoPC

To explore the contributions of TRPC5 and TRPC6 in lysoPC-induced calcium entry and inhibition of EC migration, ECs were transiently transfected with TRPC5 siRNA or TRPC6 antisense oligonucleotide to down-regulate TRPC5 or TRPC6, respectively. Transient transfection of ECs with TRPC5 siRNA for 24 h decreased the total TRPC5 level to 31 ± 2% of control (n = 3; $p < 0.02$) as shown by immunoblot analysis at 48 h (Figure 5A). Treatment with a negative control siRNA had no effect on the expression of TRPC5. ECs incubated with phosphothioate-modified TRPC6 antisense oligonucleotides for 24 h had significantly decreased total TRPC6 level, as determined by immunoblot analysis, at 48 h (Figure 5B). Treatment with sense or scrambled oligonucleotide had no effect on TRPC6 level. No change was observed in TRPC3 protein level (data not shown), indicating specificity of the TRPC6 antisense oligonucleotide.

Decreasing the level of TRPC5 or TRPC6 protein had a significant effect on lysoPC-induced increased in $[Ca^{2+}]_i$ (Figure 5, C and D). Decreased expression of TRPC5 limited the prolonged increase in $[Ca^{2+}]_i$, but a transient calcium influx occurred, the peak of which was 38 ± 2% of that in control cells (n = 3; $p < 0.0005$, Figure 5C). The lysoPC-induced rise in $[Ca^{2+}]_i$ in ECs transfected with a negative control siRNA (n = 3) was similar to that in nontransfected control ECs. Down-regulation of TRPC6 by antisense oligonucleotide had a significant effect on the lysoPC-induced rise in $[Ca^{2+}]_i$ (Figure 5D), reducing the initial rise to 27 ± 3% of the peak seen in control cells (n = 3; $p < 0.0005$). LysoPC-induced rise in $[Ca^{2+}]_i$ in ECs treated with sense or scrambled oligonucleotide was similar to control ECs (n = 3). Although variation in the methodology and effectiveness of decreasing TRPC5 and TRPC6 protein does not allow direct comparison of results, decreasing TRPC6 protein appeared to have a more profound effect on the initial rise in $[Ca^{2+}]_i$ than did decreasing TRPC5 protein.

The effect of TRPC5 or TRPC6 down-regulation on EC migration in presence of lysoPC was assessed. LysoPC inhibited migration to 35% of baseline in control ECs, but after down-regulation of TRPC5, migration in the presence of lysoPC was preserved at 51% of baseline (Figure 5E). Although slight inhibition ($p < 0.005$) of basal migration was noted in siRNA-transfected EC compared with nontransfected cells, control transfection did not alter the inhibitory effect of lysoPC. TRPC6 down-regulation limited the antimigratory effect of lysoPC, preserving migration at 61% of baseline (Figure 5F). Transfection of ECs with either scrambled or antisense oligonucleotides caused a small (10%) but significant ($p < 0.005$) decrease in EC migration, but did not alter the inhibitory effect of lysoPC. The partial preservation of EC migration in lysoPC by TRPC5 or TRPC6 down-regulation suggested their involvement in lysoPC's antimigratory effect.

Calcium Dependence of TRPC5 and TRPC6 Externalization

To determine if the lysoPC-induced TRPC6 and TRPC5 activation was dependent on $[Ca^{2+}]_i$, externalization of both channels was assessed after preincubation with intracellular calcium chelators. LysoPC-induced TRPC5 externalization was completely inhibited by preincubation with BAPTA/AM (25 μM) or EGTA/AM (30 μM; n = 5, Figure 6A, left top panel). No alterations in total TRPC5 level were identified (Figure 6A, left bottom panel). On the other hand, lysoPC-induced TRPC6 channel externalization was not inhibited by BAPTA/AM or EGTA/AM (n = 5, Figure 6A, right top panel); instead, both chelators caused increased externalization of TRPC6 and enhanced the effect of 12.5 μM lysoPC. No changes in total TRPC6 level were identified (Figure 6A, right bottom panel). These results suggested that lysoPC-induced TRPC5 translocation required free intracellular Ca^{2+}, but TRPC6 translocation was not dependent on intracellular Ca^{2+} and a decrease in free Ca^{2+} might induce TRPC6 translocation. These observations also established unique, distinguishable mechanisms for TRPC5 and TRPC6 externalization.

A potential mechanism by which lysoPC activates TRPC5 and TRPC6 channels is alteration in the plasma membrane allowing ion influx that secondarily activates TRPC channels. LysoPC-induced TRPC channel translocation was assessed in the presence and absence of extracellular calcium. LysoPC induced a 2.4 + 0.1-fold (n = 3, $p < 0.02$) increase of TRPC5 protein externalization in the presence of extracellular calcium, but no TRPC5 translocation in calcium-free buffer (Figure 6B, left panel). Total TRPC5 was not different in calcium-containing or calcium-free buffer and was not changed by lysoPC treatment (n = 3). In contrast, lysoPC

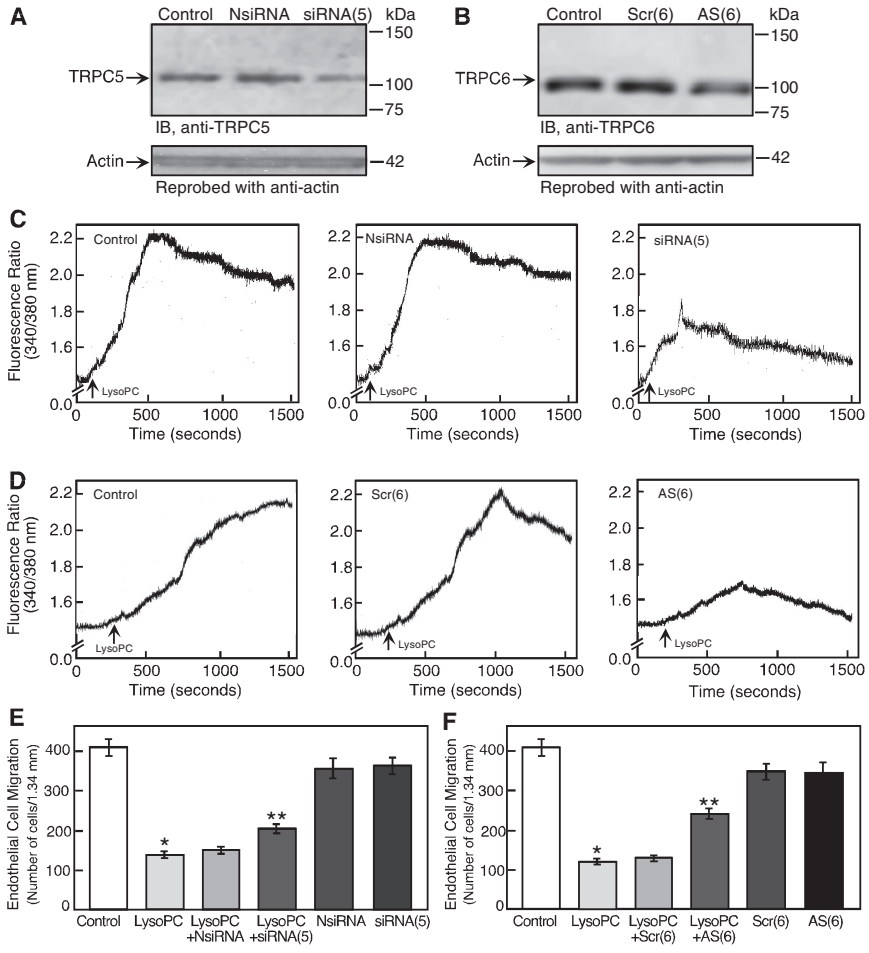

Figure 5. TRPC5 or TRPC6 down-regulation blunted the lysoPC-induced $[Ca^{2+}]_i$ rise and inhibition of migration. (A) For 24 h, ECs were incubated with negative control siRNA [NsiRNA] or siRNA targeted against TRPC5 mRNA [siRNA(5)]. ECs were then made quiescent for 24 h, lysed, and immunoblot analysis performed for TRPC5. Blots were reprobed for actin to confirm equal loading. (B) For 24 h, ECs were incubated with scrambled [Scr(6)] or antisense [AS(6)] oligonucleotide targeted against TRPC6 mRNA. Oligonucleotides were removed, and ECs were made quiescent for 24 h and then lysed, and immunoblot analysis was performed for TRPC6 (top panel). Blots were reprobed for actin to confirm equal loading (bottom panel). (C) ECs were transiently transfected for 24 h with NsiRNA or siRNA(5). The siRNA was removed and ECs were made quiescent for 12–24 h. Then ECs were loaded with fura 2-AM. After adjusting the baseline, lysoPC (12.5 μM) was added to cells (arrow), and relative change of $[Ca^{2+}]_i$ was monitored in control cells (left panel), NsiRNA-transfected ECs (central panel), or siRNA(5)-transfected ECs (right panel). (D) Similarly, ECs were transiently transfected with Scr(6) or AS(6) oligonucleotides for 24 h, made quiescent, and then loaded with fura 2-AM. LysoPC (12.5 μM) was added (arrow), and relative change of $[Ca^{2+}]_i$ was monitored in control cells (left panel), Scr(6)-transfected ECs (central panel), or AS(6)-transfected ECs (right panel). (E) ECs were transiently transfected for 24 h with NsiRNA or siRNA(5) and then made quiescent for 12 h. EC migration assay was initiated in the presence or absence of lysoPC (12.5 μM; n = 3). (F) ECs were transiently transfected with Scr(6) or AS(6) oligonucleotides for 24 h and then made quiescent for 12 h. EC migration assay was initiated in the presence or absence of lysoPC (12.5 μM; n = 4). In A–D, representative blots or traces of at least three separate experiments are shown. In E and F, results are represented as mean ± SD; *$p < 0.001$ compared with control and **$p < 0.001$ compared with lysoPC.

induced a similar increase in TRPC6 protein translocation to the plasma membrane in the presence or absence of extracellular calcium, 2.1 ± 0.5-fold (n = 3, $p < 0.02$) and 2.1 ± 0.2-fold (n = 3, $p < 0.02$), respectively (Figure 6B, right

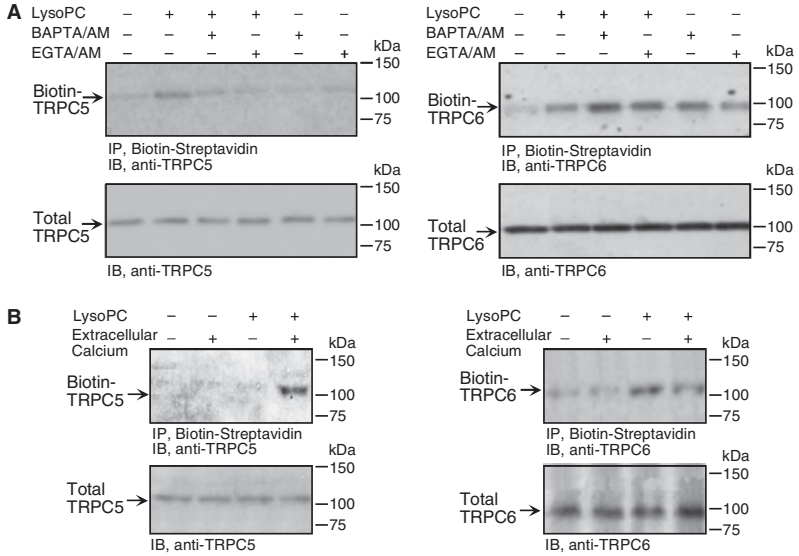

Figure 6. LysoPC-induced TRPC5 translocation is calcium-dependent, but TRPC6 translocation is calcium-independent. (A) ECs were preincubated with BAPTA/AM (25 μM) or EGTA/AM (30 μM) for 30 min before and during incubation with lysoPC (12.5 μM) for 3 min. Cell surface proteins were biotinylated, and immunoblot analysis was performed for biotinylated TRPC5 (left top panel) or TRPC6 (right top panel). Before incubation with streptavidin-agarose beads, an aliquot of cell lysate was removed for immunoblot analysis to determine total TRPC5 (left bottom panel) or TRPC6 (right bottom panel). (B) ECs were incubated with lysoPC (12.5 μM) for 30 min in the absence or presence of Ca^{2+} in KR buffer. Cell surface proteins were biotinylated, and immunoblot analysis was performed for biotinylated TRPC5 (left panel) or TRPC6 (right panel). Representative blots of five and three separate experiments are shown in A and B, respectively.

panel). Also, lysoPC-induced tyrosine phosphorylation of TRPC6 was similar in calcium-free and calcium-containing buffer (data not shown). LysoPC induced TRPC6 externalization in the absence of external calcium, but lysoPC caused no increase in $[Ca^{2+}]_i$ in the absence of extracellular calcium (Chaudhuri *et al.*, 2003), suggesting that TRPC6 activation was calcium-independent.

LysoPC Activation of TRPC5 was TRPC6-dependent

The time course of TRPC externalization depicted in Figure 2 suggested that TRPC6 is externalized in advance of TRPC5. This combined with the calcium dependence of TRPC5 externalization raised the possibility that TRPC5 externalization may depend on the opening of TRPC6 channels. The effect of lysoPC on TRPC5 externalization was assessed in *TRPC6*$^{-/-}$ MAECs. When *TRPC6*$^{-/-}$ MAEC were incubated with lysoPC for 1 h, no increase in TRPC5 externalization could not be detected by biotinylation assay (Figure 7A). This is in sharp contrast to the lysoPC-induced TRPC5 translocation observed in wild-type MAECs. Decreasing TRPC6 levels using TRPC6 antisense oligonucleotide did not change the endogenous level of TRPC5, but inhibited lysoPC-induced phosphorylation of TRPC5 (data not shown). The inability of lysoPC to externalize TRPC5 in

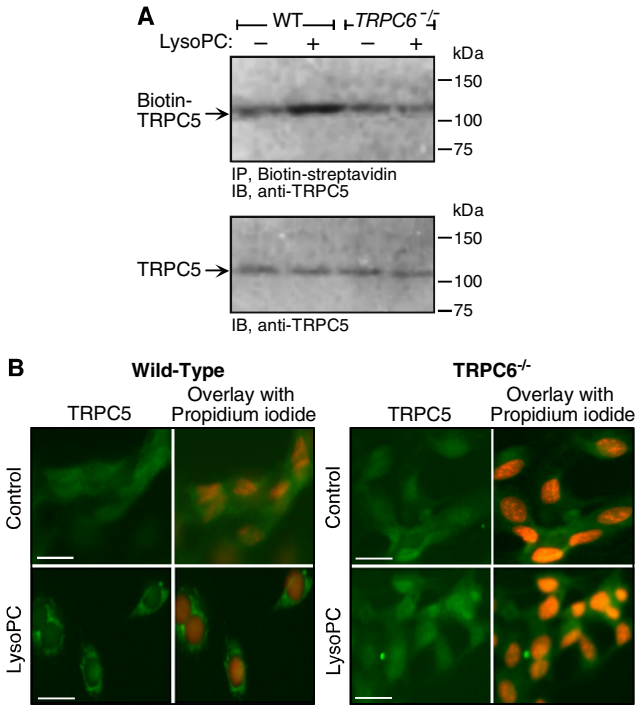

Figure 7. LysoPC-induced translocation of TRPC5 is dependent on TRPC6. (A) MAECs from wild-type (WT) and *TRPC6*$^{-/-}$ mice were incubated with lysoPC for 1 h. Cell surface proteins were biotinylated, and immunoblot analysis was performed for biotinylated TRPC5 (top panel). Before incubation with streptavidin-agarose beads, an aliquot of cell lysate was removed for analysis of total TRPC5 by immunoblot analysis (lower panel; n = 4). (B) WT and *TRPC6*$^{-/-}$ MAECs were grown to 60% confluency, washed, treated with or without lysoPC for 15 min, and then incubated with anti-TRPC5 antibody followed by Alexa 488–conjugated secondary antibody. TRPC5 location was assessed by immunofluorescence microscopy. Nuclei were detected by counterstaining with propidium iodide. The images of TRPC5 in ECs are the representative of four randomly chosen fields from each of three experiments. Original magnification, 40×. Bar, 40 μm.

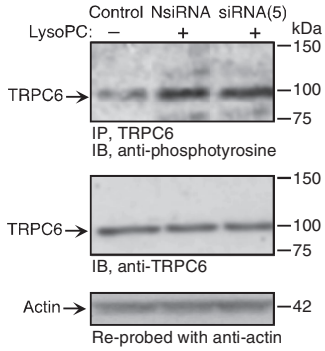

Figure 8. LysoPC-induced phosphorylation of TRPC6 is not dependent on TRPC5. ECs were incubated with siRNA targeted against TRPC5 mRNA [siRNA(5)] or negative control siRNA [NsiRNA] for 24 h. siRNA was removed and after an additional 24 h, lysoPC (12.5 μM) was added for 1 h. Then TRPC6 was immunoprecipitated, and immunoblot analysis for phosphotyrosine was performed (top panel). Similarly treated or control ECs were lysed, and immunoblot analysis for TRPC6 was performed (middle panel). Blots were reprobed for actin to confirm equal loading (bottom panel). Representative blots of three separate experiments are shown.

TRPC6$^{-/-}$ MAECs was confirmed using fluorescence microscopy after immunostaining with anti-TRPC5 and fluorescent-labeled secondary antibody. The pattern of TRPC5 protein fluorescence was diffuse throughout the cytoplasm under control conditions in both wild-type MAECs and in *TRPC6*$^{-/-}$ MAECs (n = 3, Figure 7B, top panels). After incubation with lysoPC, TRPC5 fluorescence in wild-type MAECs (n = 3, Figure 7B, bottom left panel) was associated with the plasma membrane. However, in *TRPC6*$^{-/-}$ MAECs (n = 3, Figure 7B, bottom right panel), the pattern of TRPC5 protein fluorescence after incubation in lysoPC continued to be diffuse throughout the cytoplasm, showing that TRPC5 did not translocate to the membrane. Decreasing TRPC5 levels using siRNA (Figure 8) had no effect on TRPC6 levels or lysoPC-induced phosphorylation of TRPC6 (Figure 8). The earlier translocation of TRPC6 compared with TRPC5, the distinct mechanisms of TRPC5 and TRPC6 translocation with respect to calcium requirement, and the lack of translocation of TRPC5 in TRPC6-deficient ECs suggested that lysoPC-induced TRPC5 activation was TRPC6-dependent. This unique relationship was not due to a physical association, as evidenced by lack of coimmunoprecipitation (data not shown), but possibly was secondary to an initial calcium influx caused by TRPC6 activation that subsequently activated TRPC5, allowing sustained calcium entry into ECs.

DISCUSSION

In earlier studies of EC migration, we showed that a lysoPC-induced rise in $[Ca^{2+}]_i$ caused cytoskeletal changes and inhibition of movement, but the ion channels responsible were not identified (Chaudhuri *et al.*, 2003). The present studies show that lysoPC activates endogenous TRPC channels in ECs. TRPC5 and TRPC6 are externalized in the plasma membrane with subsequent increased $[Ca^{2+}]_i$ and disruption of EC migration. TRPC6 is involved in vascular endothelial growth factor–mediated increase in vascular permeability and in EC contraction in response to thrombin (Pocock *et al.*, 2004; Singh *et al.*, 2007), but other functions of TRPC5 and TRPC6 in ECs are largely unknown. The role of TRPC5 or TRPC6 in the regulation of EC migration has not

been reported previously, and our data suggest that a TRPC6-TRPC5 activation cascade is a critical element in the inhibition of EC migration by lysoPC.

Events associated with the activation of TRPC channels include externalization and ion flux. In HEK-293 cells overexpressing TRPC5, growth factors cause the rapid translocation of TRPC5 from vesicles to the plasma membrane and increase functional TRPC5 current (Bezzerides *et al.*, 2004). Serum growth factors in EC tissue culture did not appear to influence translocation of TRPC5 and TRPC6 in our studies. Baseline localization and lysoPC-induced translocation was similar in ECs made quiescent in serum-free medium and in those maintained in 10% FBS up to initiation of experiments. TRPC6 proteins are localized in the caveolae-related microdomain vesicles, and during activation these vesicles fuse to the plasma membrane to externalize TRPC6 (Cayouette *et al.*, 2004). Tyrosine phosphorylation regulates TRPC6 activity (Hisatsune *et al.*, 2004), and increases membrane insertion of TRPC4 (Odell *et al.*, 2005), but it is not clear whether tyrosine phosphorylation is required for channel protein externalization, modification of activity, or channel opening. LysoPC induces tyrosine phosphorylation of TRPC5 and TRPC6 (Figure 1), and general tyrosine kinase inhibitors inhibit TRPC6 externalization (data not shown), suggesting that tyrosine phosphorylation is required for externalization. Although, fyn and src tyrosine kinases interact with TRPC6 to increase TRPC6 activation in COS-7 cells (Hisatsune *et al.*, 2004), the specific kinase responsible for lysoPC-induced tyrosine phosphorylation of TRPC6 in ECs has not been identified.

LysoPC activates TRPC5. In HEK-293 cells overexpressing TRPC5, lysoPC activates TRPC5, and this effect is seen even in excised membrane patches leading investigators to conclude that lysoPC has a relatively direct effect on the channel (Flemming *et al.*, 2006). Our studies suggest that in aortic ECs with only endogenous TRPC proteins, lysoPC-induced TRPC6 activation precedes and contributes to TRPC5 translocation. Down-regulation of TRPC6 in ECs inhibits lysoPC-induced TRPC5 externalization. TRPC5 can be activated by various pathways including receptor activation, external ionic activation, increased $[Ca^{2+}]_i$, and store-operated mechanisms (Zeng *et al.*, 2004). We postulate that the rise in $[Ca^{2+}]_i$ through TRPC6 channels activates TRPC5. Increased $[Ca^{2+}]_i$ can induce calcium-dependent signaling events such as myosin light-chain kinase activation that can activate TRPC5 (Shimizu *et al.*, 2006). The role of myosin light-chain kinase in lysoPC-induced activation of TRPC5 is currently under investigation in our laboratory. Interestingly, the early rise in $[Ca^{2+}]_i$ persists when TRPC5 is down-regulated using siRNA, consistent with lysoPC-induced opening of a calcium channel, such as TRPC6, and subsequent Ca^{2+} entry. In the absence of extracellular calcium, lysoPC induces the translocation of TRPC6 (Figure 6B), but $[Ca^{2+}]_i$ does not increase (Chaudhuri *et al.*, 2003), and TRPC5 is not externalized (Figure 6B). Furthermore, lysoPC does not induce TRPC5 translocation in EC preincubated with intracellular calcium chelators, BAPTA-AM or EGTA-AM, again suggesting that a $[Ca^{2+}]_i$ rise is required for activation of TRPC5 by lysoPC. The activation of TRPC5 is not simply a response to any increase in $[Ca^{2+}]_i$ because the increase in $[Ca^{2+}]_i$ secondary to bradykinin does not activate TRPC5 (data not shown). We postulate that the increased $[Ca^{2+}]_i$ must occur within specific spatial boundaries in the cell to activate TRPC5, suggesting that TRPC5 and TRPC6 are functionally connected for this unique activation cascade to occur.

Functional TRPC channels are thought to be tetramers that can be homotetramers or heterotetramers (Hofmann *et al.*, 2002). In general, endogenously expressed TRPC proteins form heteromultimers composed of members from the same subgroup (Goel *et al.*, 2002). TRPC6 and TRPC5 belong to different TRPC subgroups and are unlikely to coassemble. TRPC channels from the different subgroups can form heteromers under specific circumstances. TRPC3 and TRPC6 can form a heteromeric channel complex with TRPC1, TRPC4, and TRPC5 in rat embryonic brain but not in adult brain (Strübing *et al.*, 2003). Our coimmunoprecipitation studies suggest that TRPC5 and TRPC6 are not coassembled in a heteromeric channel (data not shown), in agreement with a previously published report (Goel *et al.*, 2005). TRPC6 and TRPC5 protein could form heteromultimers that are not identified in coimmunoprecipitation studies due to low channel density or antigenic sites hidden by heteromultimer formation. However, the correlation of TRPC6 activation with initial increase of calcium and the lag in TRPC5 activation argue against a TRPC5-TRPC6 heteromultimer and instead suggest a novel TRPC6-initiated, functional TRPC6-TRPC5 channel cascade.

Activation of a novel TRPC6-TRPC5 channel cascade plays a key role in calcium entry and inhibition of EC migration by lysoPC. A spike in $[Ca^{2+}]_i$ is needed to initiate cell movement (Tran *et al.*, 1999), but a prolonged increase, as is seen in ECs incubated in the presence of lysoPC, inhibits EC migration. Our data suggest that lysoPC initially activates TRPC6, causing increased $[Ca^{2+}]_i$ that leads to externalization of TRPC5, which allows a prolonged increase in $[Ca^{2+}]_i$ that inhibits EC migration. Down-regulation of TRPC6 inhibits TRPC5 activation, suggesting a TRPC6-dependent activation of TRPC5 by lysoPC. Although increased $[Ca^{2+}]_i$ is only one of several pathways by which lysoPC inhibits EC migration (Ghosh *et al.*, 2002; Chaudhuri *et al.*, 2005), partial preservation of migration is achieved by preventing the lysoPC-induced $[Ca^{2+}]_i$ rise. A better understanding of the TRPC6-TRPC5 activation cascade will allow development of therapeutic agents to preserve EC movement and promote angiogenesis and healing of EC injuries in atherosclerotic arteries.

ACKNOWLEDGMENTS

The authors thank Laurie Castel for her invaluable assistance with the patch clamp studies. This work was supported in part by extramural grants HL41178 and HL64357 from the National Institutes of Health (NIH), National Heart, Lung, and Blood Institute (L.M.G.) and in part by the Intramural Research Program of the NIH (L.B.).

REFERENCES

Bezzerides, V. J., Ramsey, I. S., Kotecha, S., Greka, A., and Clapham, D. E. (2004). Rapid vesicular translocation and insertion of TRP channels. Nat. Cell Biol. *6*, 709–720.

Boulay, G., Zhu, X., Peyton, M., Jiang, M., Hurst, R., Stefani, E., and Birnbaumer, L. (1997). Cloning and expression of a novel mammalian homolog of *Drosophila Transient Receptor Potential* (Trp) involved in calcium entry secondary to activation of receptors coupled by the Gq class of G protein. J. Biol. Chem. *272*, 29672–29680.

Cayouette, S., Lussier, M. P., Mathieu, E. -L., Bousquet, S. M., and Boulay, G. (2004). Exocytotic insertion of TRPC6 channel into the plasma membrane upon G_q protein-coupled receptor activation. J. Biol. Chem. *279*, 7241–7246.

Chaudhuri, P., Colles, S. M., Damron, D. S., and Graham, L. M. (2003). Lysophosphatidylcholine inhibits endothelial cell migration by increasing intracellular calcium and activating calpain. Arterioscler. Thromb. Vasc. Biol. *23*, 218–223.

Chaudhuri, P., Colles, S. M., Fox, P. L., and Graham, L. M. (2005). Protein kinase Cδ-dependent phosphorylation of syndecan-4 regulates cell migration. Circ. Res. *97*, 674–681.

Dietrich, A. *et al.* (2005). Increased vascular smooth muscle contractility in *TRPC6*$^{-/-}$ mice. Mol. Cell. Biol. *25*, 6980–6989.

Flemming, P. K., Dedman, A. M., Xu, S. -Z., Li, J., Zeng, F., Naylor, J., Benham, C. D., Bateson, A. N., Muraki, K., and Beech, D. J. (2006). Sensing of lysophospholipids by TRPC5 calcium channel. J. Biol. Chem. *281*, 4977–4982.

Ghosh, P. K., Vasanji, A., Murugesan, G., Eppell, S. J., Graham, L. M., and Fox, P. L. (2002). Membrane microviscosity regulates endothelial cell motility. Nat. Cell Biol. *4*, 894–900.

Goel, M., Sinkins, W. G., and Schilling, W. P. (2002). Selective association of TRPC channel subunits in rat brain synaptosomes. J. Biol. Chem. *277*, 48303–48310.

Goel, M., Sinkins, W., Keightley, A., Kinter, M., and Schilling, W. P. (2005). Proteomic analysis of TRPC5- and TRPC6-binding partners reveals interaction with the plasmalemmal NA^+/K^+-ATPase. Pfluegers Arch. *451*, 87–98.

Hisatsune, C., Kuroda, Y., Nakamura, K., Inoue, T., Nakamura, T., Michikawa, T., Mizutani, A., and Mikoshiba, K. (2004). Regulation of TRPC6 channel activity by tyrosine phosphorylation. J. Biol. Chem. *279*, 18887–18894.

Hofmann, T., Schaefer, M., Schultz, G., and Gudermann, T. (2002). Subunit composition of mammalian transient receptor potential channels in living cells. Proc. Natl. Acad. Sci. USA *99*, 7461–7466.

Isshiki, M., Ando, J., Yamamoto, K., Fujita, T., Ying, Y., and Anderson, R.G.W. (2002). Sites of Ca^{2+} wave initiation move with caveolae to the trailing edge of migrating cells. J. Cell Sci. *115*, 475–484.

Liu, D. *et al.* (2006). Transient receptor potential channels in essential hypertension. J. Hypertens. *24*, 1105–1114.

Lièvremont, J. -P., Bird, G. St. J., and Putney, J. W., Jr. (2004). Canonical transient receptor potential TRPC7 can function as both a receptor- and store-operated channel in HEF-293 cells. Am. J. Physiol. Cell Physiol. *287*, C1709–C1716.

Nilius, B., and Droogmans, G. (2003). Transient receptor potential channels in endothelium: solving the calcium entry puzzle? Endothelium *10*, 5–15.

Odell, A. F., Scott, J. L., and Van Helden, D. F. (2005). Epidermal growth factor induces tyrosine phosphorylation, membrane insertion, and activation of transient receptor potential channel 4. J. Biol. Chem. *280*, 37974–37987.

Okada, T. *et al.* (1999). Molecular cloning and functional characterization of a novel mouse transient receptor potential protein homologue TRP7. J. Biol. Chem. *274*, 27359–27370.

Pocock, T. M., Foster, R. R., and Bates, D. O. (2004). Evidence of a role for TRPC channels in VEGF-mediated increased vascular permeability in vivo. Am. J. Physiol. Heart Circ. Physiol. *286*, H1015–H1026.

Portman, O. W., and Alexander, M. (1969). Lysophosphatidylcholine concentration and metabolism in aortic intima plus inner media: effect of nutritionally induced atherosclerosis. J. Lipid Res. *10*, 158–165.

Shi, W., Haberland, M. E., Jien, M. -L., Shih, D. M., and Lusis, A. J. (2000). Endothelial responses to oxidized lipoproteins determine genetic susceptibility to atherosclerosis in mice. Circulation *102*, 75–81.

Shimizu, S., Yoshida, T., Wakamori, M., Ishii, M., Okada, T., Takahashi, M., Seto, M., Sakurada, K., Kiuchi, Y., and Mori, Y. (2006). Ca^{2+}-calmodulin-dependent myosin light chain kinase is essential for activation of TRPC5 channels expressed in HEK293 cells. J. Physiol. (Lond). *570*, 219–235.

Singh, I., Knezevic, N., Ahmmed, G. U., Kini, V., Malik, A. B., and Mehta, D. (2007). $G\alpha_q$-TRPC6-mediated Ca^{2+} entry induces RhoA activation and resultant endothelial cell shape change in response to thrombin. J. Biol. Chem. *282*, 7833–7843.

So, I., Chae, M. R., Kim, S. J., and Lee, S. W. (2005). Lysophosphatidylcholine, a component of atherogenic lipoproteins, induces the change of calcium mobilization via TRPC ion channels in cultured human corporal smooth muscle cells. Int. J. Impot. Res. *17*, 475–483.

Strübing, C., Krapivinsky, G., Krapivinsky, L., and Clapham, D. E. (2003). Formation of novel TRPC channels by complex subunit interactions in embryonic brain. J. Biol. Chem. *278*, 39014–39019.

Subbaiah, P. V., Chen, C. -H., Bagdade, J. D., and Albers, J. J. (1985). Substrate specificity of plasma lysolecithin acyltransferase and the molecular species of lecithin formed by the reaction. J. Biol. Chem. *260*, 5308–5314.

Tran, P.O.T., Hinman, L. E., Unger, G. M., and Sammak, P. J. (1999). A wound-induced $[Ca^{2+}]_i$ increase and its transcriptional activation of immediate early genes is important in the regulation of motility. Exp. Cell Res. *246*, 319–326.

Welsh, D. G., Morielli, A. D., Nelson, M. T., and Brayden, J. E. (2002). Transient receptor potential channels regulate myogenic tone of resistance arteries. Circ. Res. *90*, 248–250.

Yao, X., and Garland, C. J. (2005). Recent developments in vascular endothelial cell transient receptor potential channels. Circ. Res. *97*, 853–863.

Yip, H., Chan, W. -Y., Leung, P. -C., Kwan, H. -Y., Liu, C., Huang, Y., Michel, V., Yew, D.T.-W., and Yao, X. (2004). Expression of TRPC homologs in endothelial cells and smooth muscle layers of human arteries. Histochem. Cell Biol. *122*, 553–561.

Zeng, F., Xu, S. -Z., Jackson, P. K., McHugh, D., Kumar, B., Fountain, S. J., and Beech, D. J. (2004). Human TRPC5 channel activated by a multiplicity of signals in a single cell. J. Physiol. (Lond.) *559.3*, 739–750.